19. Dobrovolsky, I. P., Zubkov, S. I. and Myachkin, V. I., Estimation of the size of earthquake preparation zones. *Pageoph*, 1979, **117**, 1025–1044.
20. Molchanov, O., Schekotov, A., Fedorov, E., Belyaev, G. and Gordeev. E., Preseismic ULF electromagnetic effect from observation at Kamchatka. *NHESS*, 2003, **3**, 203–209.
21. Arora, B. R., Gahalaut, V. K. and Kumar, N., Structural control on along-strike variation in the seismicity of the northwest Himalaya. *J. Asian Earth Sci*., 2012, **57**, 15–24; doi: 10.1016/j.jseaes.2012.06.001.
22. Paul, A. and Sharma, M. L., Recent earthquake swarms in Garhwal Himalaya: a precursor to moderate to great earthquakes in the region. *J. Asian Earth Sci*., 2011, **42**, 1179–1186.
23. Trivedi, N. B., Arora, B. R., Padilha, A. L., Da Costa, J. M. and Dutra, S. L. G., Global Pc5 geomagnetic pulsations of March 24, 1991, as observed along the American sector. *Geophys. Res. Lett*., 1997, **24**, 1683–1686.
24. ftp://ftp.ngdc.noaa.gov/STP/GEOMAGNETIC_DATA/INDICES/KP_AP
25. Smirnova, N., Hayakawa, M. and Gotoh, K., Precursory behaviour of fractal characteristics of the ULF electromagnetic field in seismic active zones before strong earthquakes. *Phys. Chem. Earth*, 2004, **29**, 445–451.
26. Berry, M. V., Diffractals. *J. Phys. A: Math. Gen.*, 1979, **12**, 207–220.
27. Chamoli, A., Bansal, A. R. and Dimri, V. P., Wavelet and rescaled range approach for the Hurst exponent for short and long irregular time series. *Comput. Geosci.*, 2007, **33**, 83–93.
28. Kayal, J. R., Ram, S., Singh, O. P. and Karunakar, G., Aftershocks of the March 1999 Chamoli earthquake and seismotectonic structure of the Garhwal Himalaya. *Bull. Seismol. Soc. Am.*, 2003, **93**, 109–117; doi: 10.17851/0119990139.
29. Mahesh, P., Gupta, S., Rai, S. and Sharma, P. R., Fluid driven earthquakes in the Chamoli region, Garhwal Himalaya: evidence from local earthquake tomography. *Geophys. J. Int*., 2012, **191**, 1295–1304.
30. Israil, M., Tyagi, D., Gupta, P. K. and Sri Niwas, Investigations for imaging electrical structure of Garhwal Himalaya corridor, Uttarakhand, India. *J. Earth Syst. Sci.*, 2008, **117**, 189–200.
31. Rawat, G., Electrical conductivity imaging of Uttaranchal Himalaya using MT method. Ph D thesis, Department of Earth Sciences, IIT Roorkee, Roorkee, 2012.
32. Cicerone, R. D., Ebel, J. E. and Britton, J., A systematic compilation of earthquake precursors. *Tectonophysics*, 2009, **476**, 371–396; doi: 10.1016/j.tecto.2009.06.008.
33. Mizutani, H., Ishido, T., Yokokura, T. and Ohnishi, S., Electrokinetic phenomena associated with earthquakes. *Geophys. Res. Lett*., 1976, **13**, 365–368.
34. Dudkin, F., Rawat, G., Arora, B. R., Korepanov, V., Leontyeva, O. and Sharma, A. K., Application of polarization ellipse technique for analysis of ULF magnetic fields from two distant stations in Koyna–Warna seismoactive region, West India. *NHESS*, 2010, **10**, 1–10; doi:10.5194/nhess-10-1-2010.
35. http://www.imd.gov.in/section/seismo/dynamic/last-monthJun11.htm

ACKNOWLEDGEMENTS. I thank the Director, Wadia Institute of Himalayan Geology, Dehradun for the necessary support to carry out the work. Financial support from MoES to the MPGO-EPR project through MoES/P.O.(Seismo)/NPEP(15)/2009 is acknowledged. I also thank Dr B. R. Arora (former Director, WIHG) for guidance and motivation and the anonymous reviewers for their critical reviews and suggestions.

Received 3 August 2013; revised accepted 11 November 2013

Large capacity reaction floor-wall assembly for pseudo-dynamic testing at IIT Kanpur and its load rating

Durgesh C. Rai[1,*], Sudhir K. Jain[2], C. V. R. Murty[3] and Dipanshu Bansal[4]

[1]Department of Civil Engineering, Indian Institute of Technology Kanpur, Kanpur 208 016, India
[2]Indian Institute of Technology Gandhinagar, Ahmedabad 382 424, India
[3]Indian Institute of Technology Jodhpur, Jodhpur 342 011, India
[4]Department of Civil Engineering, State University of New York at Buffalo, USA

The earthquake simulation on full-scale civil engineering structures in a pseudo-dynamic testing facility provides an affordable and practical means to understand the seismic behaviour of structures as it provides accurate information about their real time response of inelastic behaviour up to failure. One such pseudo dynamic testing facility is nearing completion at IIT Kanpur, which has 15 m × 10 m L-shaped and 10.5 m high reaction wall and 1.2 m thick top slab of the box girder for the strong floor. The anchor points are located in the wall and floor in a square grid of 0.6 m with each point has load capacity of 1.7 MN in tension and 1.0 MN in shear. The 2 m thick post-tensioned wall using Freyssinet 12K15 cable system in a novel configuration can resist an overturning moment of 12.7 MNm per metre of the wall. The capacity of the reaction assembly depends upon number of loads applied, combination of loads and interaction between different components of the reaction assembly structure. A methodology based on 'influence coefficients' was developed to estimate the worst load combination for describing load rating of the reaction structure. Finite element analyses in ABAQUS environment were conducted to compute the influence coefficients matrix whose elements can be added linearly to find out the maximum loading effect on the reaction structure which can be used to determine the limiting load for a particular case of load application.

Keywords: Pseudo-dynamic testing facility, reaction wall, seismic behaviour, load rating.

THE survival of conventional structures during earthquakes depends on their ability to deform inelastically and dissipate seismic energy. The performance evaluation of their energy dissipation potential is difficult by analytical methods due to their complex inelastic behaviour. As a result, experimental testing is most commonly employed to study the inelastic behaviour of structures in earthquake-type loads. The pseudo-dynamic test (PDT) is an experimental technique for simulating the earthquake response of structures and structural components in time

*For correspondence. (e-mail: dcrai@iitk.ac.in)

domain using on-line computer controlled tests[1,2]. The method offers a reliable, economic and efficient experimental assessment of the structural behaviour of large-scale structures and their components.

The PDT procedure is a simultaneous simulation and control process in which inertia and damping properties are taken into account in the virtual sense. The test structure is idealized as a discrete parameter system, so that equations of motion are a set of ordinary differential equations, which can be solved by time-stepping methods in real time, efficiently and accurately. Any structural analysis programs capable of nonlinear analysis such as OpenSees or DRAIN family of programs can be employed for idealizing the test structures[3,4]. In this procedure stiffness properties are acquired from the real model of the structure only by directly measuring the restoring forces. Based on active control theory, dynamic displacements are calculated using the simulated inertia, damping and acquired stiffness properties for a particular ground motion, and the response of the structure is simulated under seismic motion in a quasi-static fashion[5]. Various components of the test method are schematically shown in Figure 1. Equations of motion are solved on-line for displacements to be applied in real time by a step-by-step numerical integration method while updating the system parameters from on-line measurements of restoring forces and displacements. Effect of inertia force is accounted for in approximate sense and strain rate effects are not considered as the test is carried out at a slow rate[6]. Closed-loop servo-controlled hydraulic actuators are used to apply displacements with the help of a PID servo-controller. These imposed displacements on the test structure will resemble those if the structure were tested under real-time dynamic conditions.

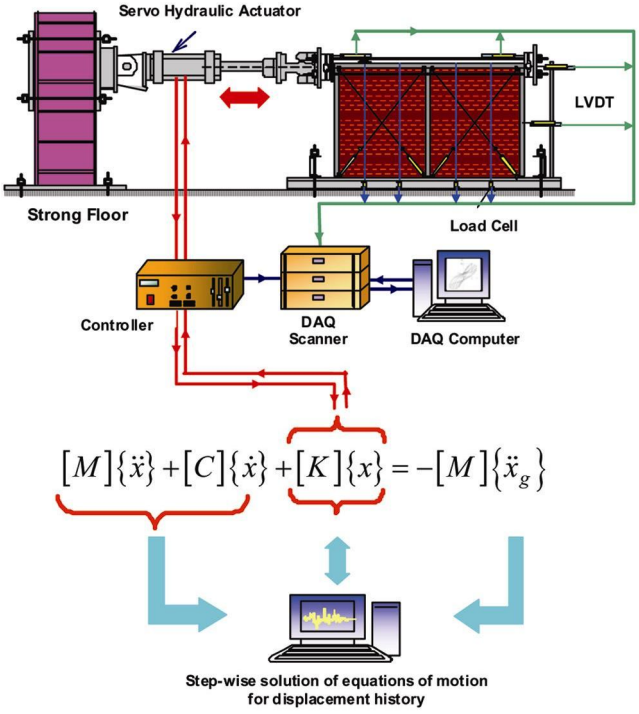

Figure 1. Pseudo-dynamic testing method and components.

The exact simulation of the earthquake motion to full or large-scale structures has been a challenge to structural engineering researchers. Table 1 summarizes some of the existing pseudo-dynamic testing facilities with their geometric dimensions and configurations of reaction walls[7]. Greater the size of the wall, larger is the specimen which can be tested without downscaling; the number of walls decides whether multi-directional experiments are possible; and the capacity of walls decides the amount of load that can be applied to the structure to get a desirable response.

The capacity of the strong reaction wall-floor assembly is the maximum load it can carry without the cracking limit of concrete being exceeded. The capacity of the reaction assembly is not only dependent on total magnitude of the applied loads, but on the number of loads applied, combination of loads and interaction between different parts of the reaction assembly. To calculate the worst load combination, which would define the capacity for each loading pattern, a methodology based on 'influence coefficients' has been developed.

For the study of prototypical (full-scale) behaviour of structures under earthquake-type loads, a pseudo-dynamic testing facility (PDTF) is nearing completion at the Department of Civil Engineering, Indian Institute of Technology Kanpur (Figure 2). This communication discusses the unique design and construction features of its reaction wall and floor assembly and a method to express the loading capacity (load rating) of such a testing facility.

The design parameters of IIT Kanpur facility are so chosen to create a moderate-size facility with a large loading capacity to provide the needed versatility for a variety of experimental options and test specimens. The overall size of various components was restricted by space constraints as it is built next to the existing strong floor and is surrounded by buildings on all sides. The *L*-shaped reaction wall, 15 and 10 m long in two perpendicular directions and 10.5 m high, can be used to test prototype size structures as large as typical three-storey buildings. The two reaction walls will facilitate bi-axial loading in the horizontal plane. Figure 2 shows the schematic arrangement and a view of the facility. The cross-sectional view and dimensions of the reaction wall-floor assembly are shown in Figure 3. The strong floor is a large stiffness three-cell box girder with the loading top slab of 1.2 m thickness in reinforced concrete. The anchor points in the strong floor are in the same square grid pattern of 0.6 m with over 1100 tie-down points for fixing the test specimen and attaching the loading equipment. The facility is housed in a 15 m tall test hall building which is served by 200 kN EOT and hard

Table 1. Some pseudo-dynamic facilities and their dimensions and configurations

Institution	Reaction wall height (m)	Strong floor area (m^2)	Reaction wall configuration
Building Research Institute (Japan)	25	600	*L*-shaped
Hazama Technical Research Institute, Hazama Corp Ltd (Japan)	18	423	*L*-shaped
European Laboratory for Structural Assessment – JRC Ispra (Italy)	16	281	Rectangular
Structural Systems Laboratory, University of California at San Diego (USA)	15	946	Rectangular
National Center for Research on Earthquake Engineering, Taipei (Taiwan)	6–15	1800	*L*-shaped stepped
Earthquake Engineering Research Centre, University of California, Berkeley (USA)	13.3	590	Reconfigurable
University of Minnesota, Minneapolis (USA)	12	297	*L*-shaped
Ecole Polytechnique, Montreal (Canada)	10	500	*L*-shaped
Protective Engineering Laboratory, Nanyang Technological University, Singapore	6–8	700	*L*-shaped stepped
University of Patras (Greece)	5.5	288	*L*-shaped

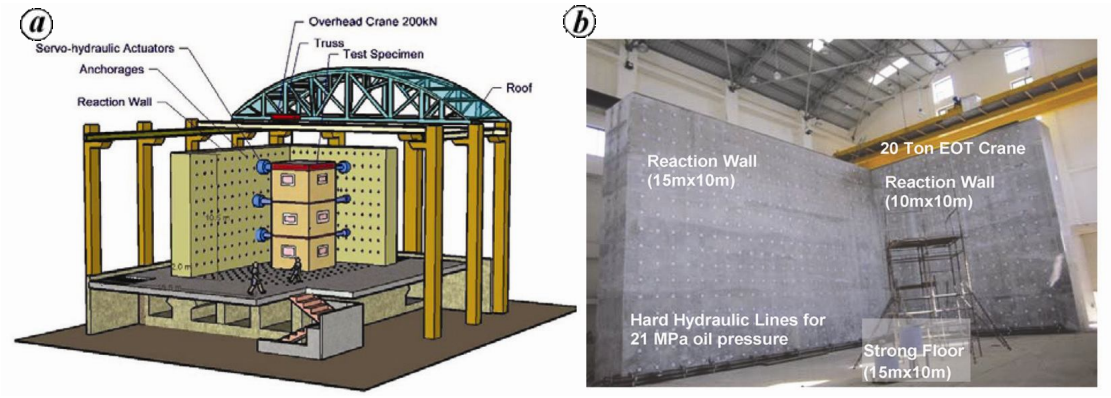

Figure 2. ***a***, Schematic diagram showing various components of PDTF. ***b***, A view of the reaction wall-floor assembly of PDTF at IIT Kanpur.

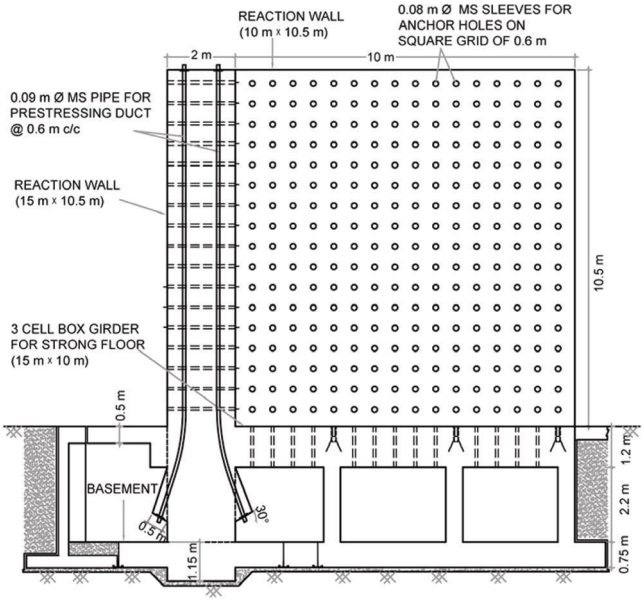

Figure 3. Cross-sectional view and dimensions of the reaction wall-floor assembly of PDTF at IIT Kanpur.

hydraulic lines of 21 MPa oil pressure rating to power servo-controlled electro-hydraulic actuators for the load application. Provisions are made in the basement to house a hydraulic pump of flow capacity as high as 1000 lpm.

Tension cracks are highly undesirable in such type of facility to maintain its integrity during the service life. Post-tensioning in the reaction walls will ensure that no tension cracks develop in concrete under the action of design loads. To ensure that the reaction walls do not experience large tensile stress and remain uncracked, the full pre-stressing was attempted by post-tensioning the walls in a novel configuration. The vertical pre-stressing of the reaction wall was achieved by post-tensioning of cables in the vertical plane, which were curved outward in the bulged portion of wall below the strong floor slab to provide access at the bottom end of the cables as well. The cables of low relaxation seven ply strands were tensioned by positioning the jacks at the top of the reaction wall and all 88 cables at 0.6 m on centres were pre-tensioned in a pre-determined sequence to gradually achieve a uniform prestress of 3.5 MPa after losses[8,9]. Figure 4 shows the general arrangement of the reaction wall-floor assembly, the ducts for post-tensioning cables and its positioning during the construction phase.

The design values of various components and properties of various materials have been summarized in Table 2. About 1000 m^3 of M45 concrete was placed in the reaction wall-floor assembly under strict quality control at the time of mixing at the plant and pouring at the site. The concrete had a mix of 0.285 : 1.000 : 0.875 : 2,276 (water : cement : fine aggregates : coarse aggregates)[10]. The

Table 2. Specifications and characteristics of PDTF at IIT Kanpur

Wall and floor specifications	
Type	*L*-shaped
Reaction wall A	15 × 10.5 × 2 m
Reaction wall B	10 × 10.5 × 2 m
Strong floor	15 × 10 × 4 m, three-cell box girder
Foundation type	Raft (0.75 m in depth)
Anchor points	0.6 m square grid
Post-tensioning system	
Anchorage system	Freyssinet-12K15
Post-tensioning cables	12 stranded cables, 15.2 mm diameter
Cable force	2430 kN
Jack type, maximum force and stroke	Multi-strand K350, 3065 kN and 250 mm
Strand type	Uncoated stress-relieved low-relaxation, seven-ply strand conforming to IS 14268: 1995 (class II, 15.2 mm dia., 140.0 mm^2 section area, 260.7 kN breaking load and 234.6 kN 0.2% proof load)
Concrete and reinforcement materials	
Concrete grade	M45 in reaction wall-floor assembly
Reinforcement	Fe415 grade TMT bars with main reinforcement in 32, 25 and 16 mm diameter bars.

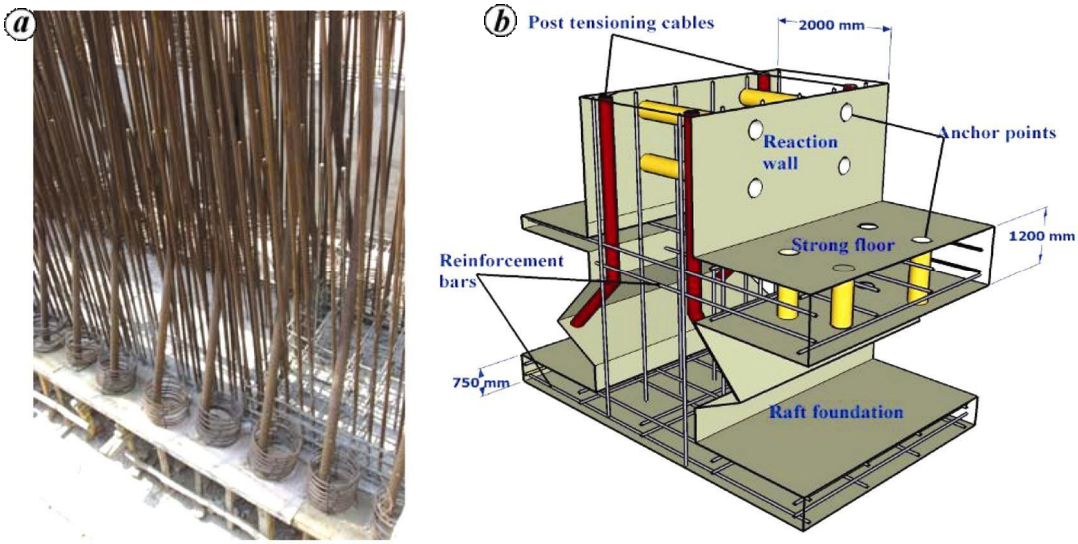

Figure 4. Arrangement of post-tensioning system for reaction walls. ***a***, Placement of ducts for post-tensioning cables during construction phase. ***b***, Cross-section of the wall showing typical arrangements of main reinforcements, anchor points and post-tensioning cables.

reinforcement bars were deformed thermo-mechanically treated (TMT) of the grade Fe415, procured from reputed manufacturers[11]. Mechanical couplers were used for splicing large diameters bars (32 mm main reinforcement) instead of more common lapping of bars. The walls and floor are heavily reinforced in two layers near each face in both directions.

The reaction walls are essentially designed as vertical cantilevers with about 0.54% steel reinforcement at each face for a large moment capacity, which is further enhanced by vertical pre-stressing. Moreover, due to continuity provided at the junction of *L*-shaped walls, significant flexure strength exists in the horizontal direction as well. The design axial force-moment (*P*–*M*) interaction curve for the wall cross-section has been obtained as shown in Figure 5, which indicates about 80% increase in design moment capacity due to pre-compression caused by post-tensioning cables. The reaction walls as vertical cantilevers have design overturning moment capacity of 12.7 MNm/m run of the wall assuming typical partial safety factors of the reinforced concrete design[12]. Table 3 summarizes the moment and shear capacity of the reaction wall and strong floor.

Worst load combination is an important parameter in deciding the load capacity of any structure. No explicit approach is available for the calculation of worst load combination for such facilities. In general practice, maximum load that can be applied to the structure is

Table 3. Load rating of strong reaction wall and test floor

Reaction wall	
Pre-stress due to vertical post-tensioning of walls after losses	3.5 MPa
Shear capacity of walls	7.4 MN/m
Moment capacity along the length of the wall (including post-tensioning effects)	12.7 MNm/m
Moment capacity along the height of wall A	5.7 MNm/m
Moment capacity along the height of wall B	5.0 MNm/m
Test floor	
Punching shear strength due to concrete only	14.49 MN
Punching shear strength due to reinforcement only	3.48 MN
Maximum load applied at each hole	1.7 MN
Maximum load applied at each hole directly above the basement wall	4.0 MN
Maximum strip load capacity at edges	9.0 MN

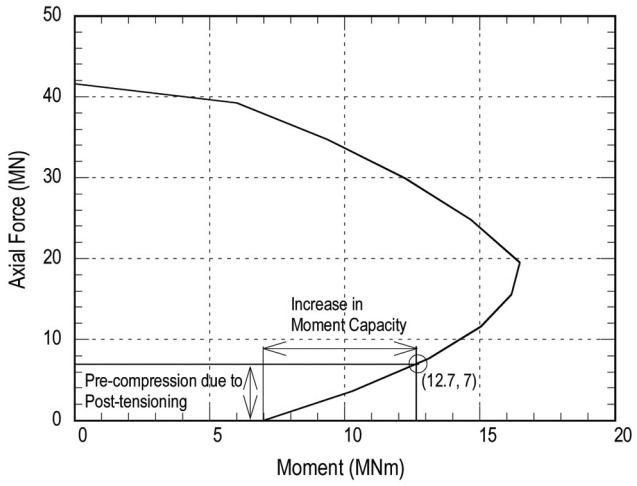

Figure 5. Axial force-moment interaction curve for the wall cross-section per metre length.

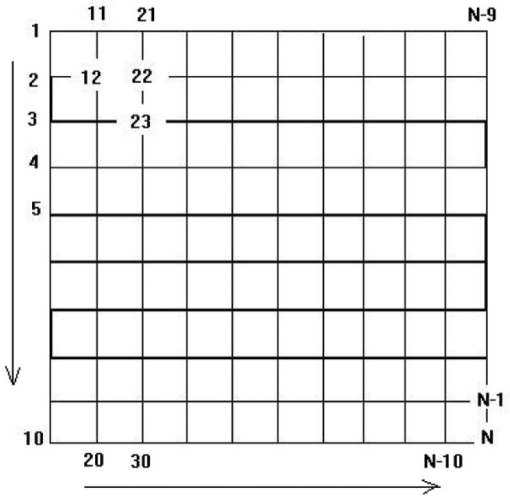

Figure 7. Grid showing the numbering of nodes in the MATLAB code.

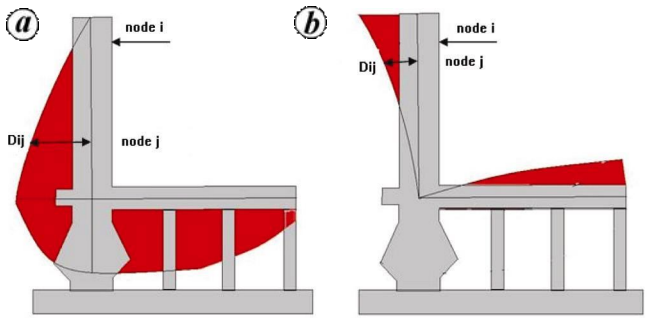

Figure 6. Response of reaction wall-floor assembly due to unit force: ***a***, stress; ***b***, displacement.

estimated for few load cases and then selecting the worst governing load case for design. Moreover, the worst load combination effect varies with the number of loading points, relative proportion of these loads and their location of the structure. To include the effect of the above-mentioned parameters, one method was to consider the influence of individual point loads and then superimpose them to obtain the cumulative effect of a particular load combination. A matrix of influence coefficients will provide the maximum load that can be applied for that particular combination of load by taking into account the maximum effect that it will generate at any location (or node). This is the motivation for calculating the influence coefficients for applied load at each wall, and estimating the maximum possible load that can be applied at nodes. Figure 6 shows how a normal stress component and out-of-plane displacement varies in structure if a unit force is applied at a given node and it represents the influence of a unit force applied at given node on stress and displacements at various other nodes of the structure.

Stress influence coefficient D_{ij} represents the magnitude of stress developed at the jth node (point) due to a unit load applied at the ith node (point) on the reaction wall. A four-dimensional matrix D_{ij} can be formed by applying unit load at each node and noting down the stress generated at different nodes. In this approach, the structure is assumed to be linear which follows the superposition principle. In other words, the direct addition of influence coefficients is possible if the load is applied at two or more nodes. For example, consider the grid shown in Figure 7, and assume that the loads are applied at nodes 1, 2, 5, 12 and N. Then using the superposition

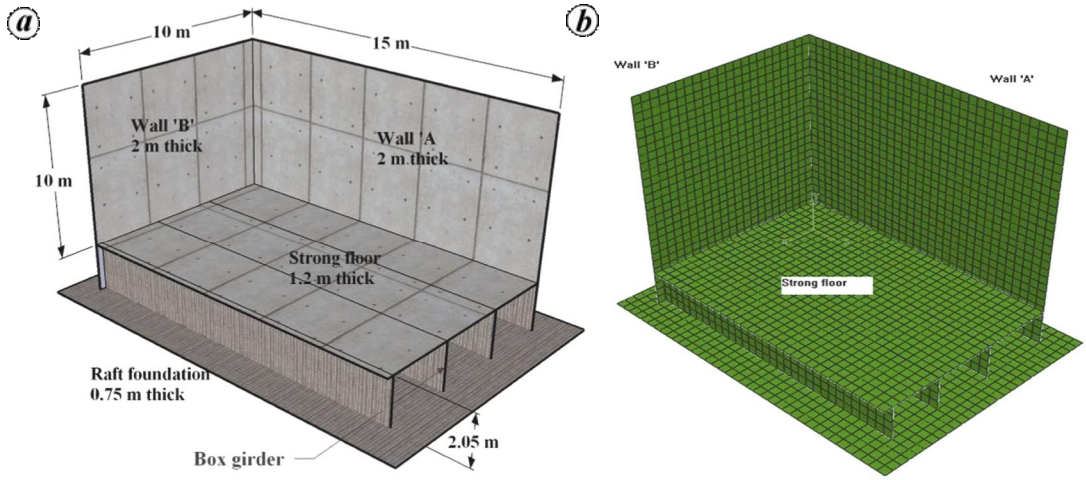

Figure 8. ***a***, Dimensions and arrangement of various parts in the Abaqus model. ***b***, Structured meshing of the structure.

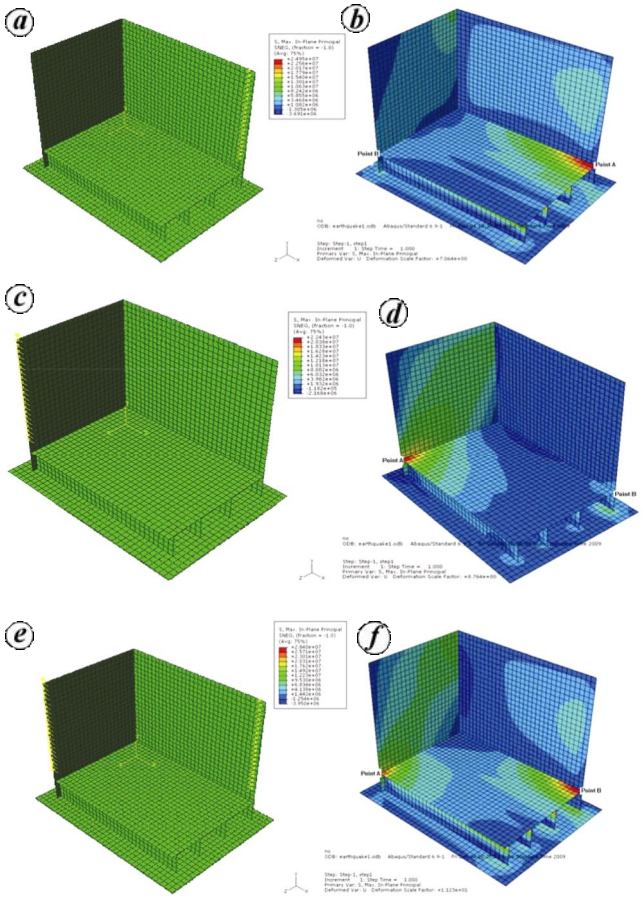

Figure 9. Stress distribution in the structure for different types of loading.

principle, the sum of influence coefficients at the jth node will be $I_j = D_{1j} + D_{2j} + D_{5j} + D_{12j} + D_{Nj}$. The maximum influence coefficient at these nodes will be simply the largest of I_j's for $1 \le j \le N$, which will be considered as a limit to maximum load that can be applied at those five nodes.

In this way, it can be seen that the maximum stress does not always occur at points which seem to be critical. A MATLAB code has been written for the facility at IIT Kanpur, which will compute the maximum value of influence coefficient with inputs of proportional ratios of applied loads at particular nodes[13]. The output will be the maximum load that can be applied at the given nodes so that the maximum tensile stress does not exceed 3.5 MPa at any node (anchor location) in the reaction wall-floor structure. Corresponding limits for compressive stress and out-of-plane displacement have not been specified, but they usually remain well below the safe limits of 20 MPa and 25 mm respectively. The program can be suitably altered for any other facility for its arrangements of anchor points for load application.

In order to get the influence coefficient matrix, finite element (FE) analyses of the reaction wall-floor assembly were performed under Abaqus environment[14]. All the structural elements (reaction wall, strong floor, stiffener, etc.) were modelled as shell elements (S4R). Materials used in defining the model have been assumed to be homogeneous and behave linearly with elastic modulus, density and Poisson ratio of the concrete and steel reinforcement as 33.5 GPa, 2400 kg/m^3, 0.2 and 200 GPa, 8000 kg/m^3, 0.3 respectively. The reinforcements in structure have been modelled by REBAR option. To transfer the load from one surface to another, node-to-node connections have been defined between various surfaces and have been modelled using TIE command. (This option is used to impose tie constraints, cyclic symmetry constraints, or coupled acoustic–structural interactions between pairs of surfaces.) Raft foundation and soil interaction have been modelled by the option of Elastic Foundation with stiffness constant of the soil as 15,000 kPa. The elastic foundation assumes that it will carry the load proportional to stiffness if in compression, but will take zero load if in tension. To get the desirable response of various structural elements, structured meshing was used for

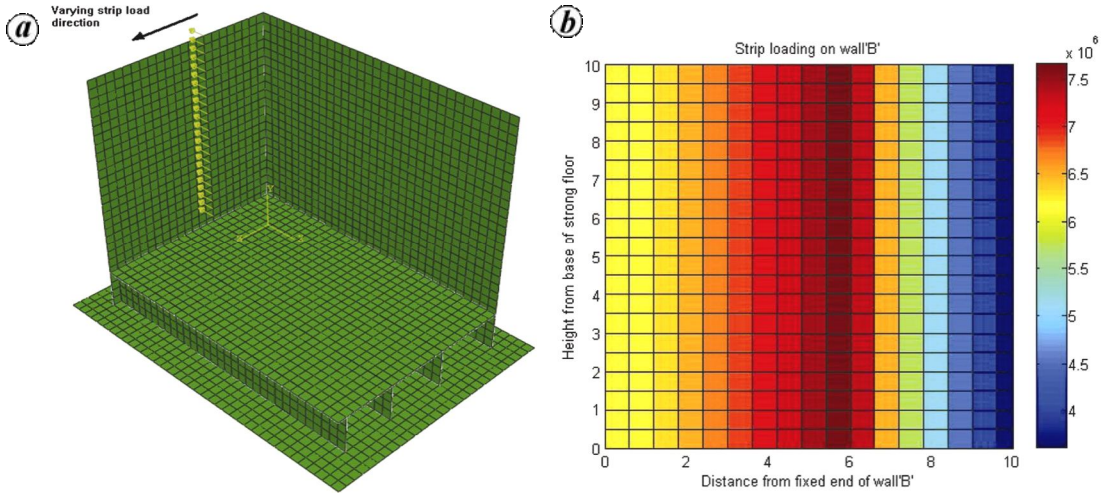

Figure 10. ***a***, Loading pattern on the reaction walls. ***b***, Load rating chart indicating the amount of load (in N) that can be applied on vertical strip of wall B.

individual parts with 0.5 m maximum element size, as shown in Figure 8. No plastic properties of the model were defined as the structure has been designed in such a way that it always remains in elastic range. To simulate the effect of quasi-static loading, static analysis has been carried out to find stresses in the structural elements.

For the no cracking condition in the reaction walls and strong floor, the concrete stress must not exceed the tensile strength of concrete. The resistance to cracking in the reaction wall is due to combined effect of pre-stressing and normal tensile strength of concrete; while in the strong floor it is simply normal tensile strength of plain concrete. For the serviceability limit of the structure, the permissible tensile stress in the concrete of the reaction walls and strong floor was taken as 3.5 MPa, assuming a safety factor of 1.35 on the modulus of rupture of concrete. Analyses indicate that the permissible concrete tensile stress governs the load-carrying capacity of the reaction wall and floor assembly, and the maximum compressive stress and out-of-plane displacement remains much below its permissible limit of 20 MPa and 25 mm respectively.

Maximum load applied at each hole, or in a horizontal/vertical strip can be found using the MATLAB code as described above. Stress profile for some of the load cases is shown in Figure 9. It can be observed that the stress concentration is maximum at points *A* and *B*, as shown in Figure 9 *b* and *d* respectively. However, if the load is applied as a combination of the above two cases, it is observed that the maximum stresses are reached at several points, including some of the points on the box girder floor as well. In such a case, the maximum load will be limited by maximum stress developed at all possible points, which may not essentially be the maximum stress condition for the individual load cases. There are many load combinations where increasing the load actually decreases the effective stress value because of mutual cancellation of compressive and tensile stresses. In those cases, the magnitude of the load can be increased at the nodes.

Using the influence coefficients, the load capacity chart as shown in Figure 10 can be prepared for one particular load case of vertical strip loading of one of the walls. It can be observed that the maximum capacity of wall B is obtained when the vertical strip load is applied at a distance of 6 m from the wall junction. Similarly, for any arbitrary loading pattern, the MATLAB code can be used to compute the magnitude of loads in that pattern.

The bi-directional reaction wall and strong floor assembly at IIT Kanpur can be used to test full-scale, large, civil engineering structures under earthquake-type loads using pseudo-dynamic technique. Two strong reaction walls of 10 m × 10.5 m and 15 m × 10.5 m provided at a corner of the strong floor of 10 m × 15 m provide ample space for placing the test specimen and loading apparatus. The design overturning moment and shear capacity per metre length of post-tensioned walls are 12.7 MNm and 7.4 MN respectively. Strong floor has the maximum tension capacity of 1.7 MN/anchor hole, limiting the maximum strip load to 9.0 MN. However, directly above the basement walls the tension capacity of each hole increases to 4.0 MN. These values are comparable with the typical values reported for such large capacity testing facilities in other countries.

A methodology of influence coefficients can be used to calculate worst load combination for the wall-floor reaction assembly. Once the matrix of influence coefficients is formed after FE analyses of the structure, all required parameters can be evaluated using superposition principle for linear behaviour of the reaction assembly. The load rating chart prepared by this technique can be used to safely position loading actuators and supports on the

reaction walls and floor. For any arbitrarily load combination, the MATLAB code developed for the purpose can be used to find the optimized load and position of the actuators.

It is expected that the information presented here will encourage commissioning of more such large-scale facilities, which will help boost experimental earthquake engineering in the country for the development and performance verification of earthquake-resistant techniques and construction types.

1. Mahin, S. A. and Shing, P. B., Pseudo-dynamic method for seismic testing. *J. Struct. Eng.*, 1985, **111**, 1482–1503.
2. Takanashi, K. and Nakashima, M., Japanese activities on online testing. *J. Eng. Mech.*, **113**, 1014–1032.
3. McKenna, F., OpenSees: a framework for earthquake engineering simulation. *Comput. Sci. Eng.*, 2011, **13**, 58–66.
4. DRAIN: A general purpose computer program for static and dynamic analyses of inelastic structures, avaliable at http://nisee.berkeley.edu/software/ (accessed on 13 November 2013).
5. Mahin, S. A., Shing, P. B., Thewalt, C. R. and Hanson, R. D., Pseudo-dynamic test method: current status and future directions. *J. Struct. Eng.*, **115**, 2113–2128.
6. Donea, J. and Jones, P. M., *Experimental and Numerical Methods in Earthquake Engineering*, Kluwer, The Netherlands, 1991.
7. Calvi, G. M., Pavese, A., Ceresa, P., Dacarro, F., Lai, C. G. and Beltrami, C., *Design of a Large-scale Dynamic and Pseudo-dynamic Testing Facility*, IUSS Press, IUSS, Pavia, Italy, 2005.
8. IS: 14266. Uncoated stress relieved low relaxation seven-ply strand for prestressed concrete-specification. Bureau of Indian Standards, New Delhi, 1995.
9. IS: 1343. Code of practice for prestressed concrete. Bureau of Indian Standards, New Delhi, 1980.
10. IS: 10262. Recommended guidelines for concrete mix design. Bureau of Indian Standards, New Delhi, 1982.
11. IS: 1786. Specification for high strength deformed steel bars and wires for concrete reinforcement. Bureau of Indian Standards, New Delhi, 2008.
12. IS: 456. Plain and reinforced concrete – code of practice. Bureau of Indian Standards, New Delhi, 2000.
13. The MathWorks. MATLAB v 7.10.0, Natick, MA, USA, 2010.
14. Simulia. ABAQUS v6.9-1, Dassault Systems Simulia Corporation, Providence, RI, USA, 2010.

ACKNOWLEDGEMENTS. The PDTF at IIT Kanpur was sponsored by the Department of Science and Technology, New Delhi through a grant under the scheme of Fund for Improvement of S&T Infrastructure (FIST). It was further supported by laboratory grant from National Program on Earthquake Engineering (NPEE) of the Ministry of Human Resource and Development, New Delhi. Generous support from IIT Kanpur for the construction of reaction wall-floor assembly and various equipment is gratefully acknowledged. The structural engineers and architects for the project were M/s Tandon Consulting Pvt Ltd, New Delhi, and Kanvinde Rai and Chowdhury, New Delhi respectively. The supervision and project management was by Institute Works Department of IIT Kanpur under the leadership of Mr Rajeev Garg.

Received 29 October 2013; revised accepted 20 November 2013